Effect of PyC interlayer amorphisation on the thermal conductivity of SiC/SiC composites

Loïc Fave[a,*], Manuel A. Pouchon[a]

[a] *Laboratory for Nuclear Materials, Paul Scherrer Institut, Villigen, Switzerland*

Abstract

During the last two decades, silicon carbide based ceramic composites (SiC/SiC) have become a candidate material for nuclear fuel cladding, first for advanced nuclear systems, such as the GFR, and recently also as potential replacement material for nuclear fuel cladding in light water reactors. This work is contributing to the General Atomics/Westinghouse led CARAT project. This paper focuses on the consequences of the microstructural changes occurring at the pyrolytic (PyC) carbon interphases linking silicon carbide matrix and fibres in the composite.

The experimental approach is two-fold: measurements of the thermal conductivity of short sections of prototype SiC/SiC cladding tubes deal with the macro-scale of the question, whereas the effects of radiation damage on the PyC interlayer are studied by energy filtered transmission electron microscopy (EFTEM) as well as spectrum imaging in STEM (ESI).

The results from both parts of the experimental work are brought together in an effective medium model based on the work of Markworth and Youngblood et al. [1,2]. A detailed outlining of the radial heat flow [3] experimental apparatus developed to this end has been presented at the 2016 ANS meeting in New Orleans [4].

Keywords: Thermal conductivity, SiC/SiC, continuous medium modelling, pyrolytic carbon, radiation damage

1. Introduction

Silicon carbide is considered to be one of the future structural materials for nuclear applications. It shows a rather tolerant behaviour under irradiation and is chemically inert in most environmental conditions foreseen for such systems. Except for its lack of ductility, this ceramic has excellent mechanical properties up to very high temperatures. Here, silicon carbide is considered as a replacement material for Zircaloy in LWR cladding, or as cladding for future reactor systems, such as the gas cooled fast reactors (GFR). The motivation for replacing zircaloy in LWRs comes from an initiative aiming at reducing the chemically reactive volume in the core by changing for inert systems. This is generally known as a part of accident tolerant fuel (ATF) research efforts, which is often accompanied by a change of fuel system (U-N, U-Si or U-C).

Since ductility is an essential property for cladding applications, SiC/SiC composite materials are being looked at instead of monolithic SiC bodies. Another essential feature is water and gas tightness of the clad. As ceramics matrix are partly porous and have small cracks, this aspect has to be ensured by either having additional layers of monolithic ceramic, or with a metallic liner. A major question arising from the rather complex structure of these multilayered tube concept is that of the effective thermal conductivity, and if it suffices to limit the fuel temperature to reasonable values.

All of the designs studied in this work include several of the aforementioned layers, so that gas and water tightness might be achieved: some of these layers are made of SiC/SiC composite, whereby granting suitable mechanical properties to the assembly, whilst others grant the tightness. To correctly account for the various parameters affecting thermal transport in such systems, the modelling has to consider two scales. Firstly, the effective thermal conductivity of the composite layers has to be determined, including effects such as irradiation induced changes and structural defects like porosity. This can then be used to calculate the actual thermal conductivity of the assembly which is modelled as a cylindrical series of thermal resistances.

Being a graphite like carbon, the PyC used for the fiber/matrix interphase is known to suffer from microcracking [5], amorphisation [6] and dimensional changes through swelling as well as the so-called Wigner effect [7,8]. Partial amorphisation of the interphase has been observed in irradiated material by studying the carbon K-edge in EFTEM and STEM-EELS, meaning that a change of its thermal properties will ensue. Carbon allotropes are known to span an extraordinarily large range of thermal conductivities: from sub-unity values in amorphous carbons up to 10'000 $W \cdot m^{-1} \cdot K^{-1}$ in diamond [9].

*L. Fave (✉), Laboratory for Nuclear Materials, 5232 Villigen, Switzerland, e-mail: loic.fave@alumni.epfl.ch

Reprint available online:
• infoscience at EPFL: https://infoscience.epfl.ch/record/224383
• e-collection at ETHZ: http://dx.doi.org/10.3929/ethz-a-010810098

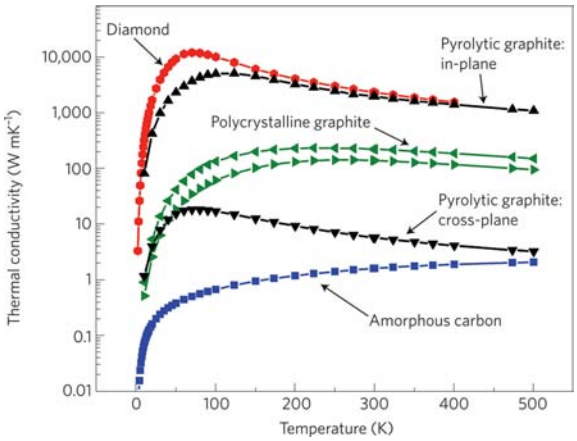

Figure 1: Thermal conductivity of carbon allotropes: amorphous carbon, pyrolytic and polycrystalline graphite and diamond. Reproduced from Balandin's paper [9].

Including these considerations in a Markworth model, we show that amorphisation of the PyC interlayers will lead to further reduction of the thermal conductivity which needs being accounted for.

2. Theory

2.1. Continuous medium modelling

The modelling approach followed in this paper is the one presented by Markworth [1], where unidirectional composites, on which a transverse temperature gradient is applied, are considered.

Figure 2 shows a schematic view of the geometry at hand.

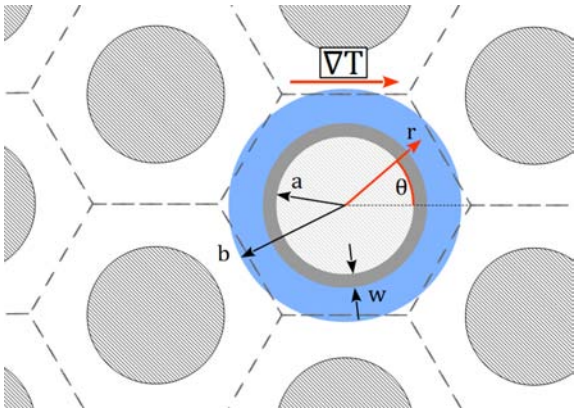

Figure 2: Schematic view of the SiC/SiC composite structure, with fibres (hatched), interphase layer (grey) and matrix (blue).

The analysis is based on a set of parameters listed below:

- SiC fibres with a diameter $2a$ are considered homogeneously distributed
- A PyC layer of thickness w is deposited on the surface of the fibres
- A given volume of matrix can be attributed to each fibre as a concentric cylinder with a diameter $2b$ according to the fibre volume fraction V_f.
- The volume fraction of fibres is $V_f = \left(\frac{a}{b}\right)^2$
- A temperature gradient $\vec{\nabla} = \begin{pmatrix}\Delta T & 0 & 0\end{pmatrix}$ is applied on the composite, i.e. the actual cladding tubes are heated from the inside.
- The ensemble formed by a fibre, its interlayer and attributed matrix volume is used to form hexagonal Wigner-Seitz cells whose area is equivalent to the circular area presented in Figure 2.

In this situation, the temperature distribution in the composite was described by Rayleigh [10]:

$$T_i = A_i + \left(\frac{B_i}{\rho} + C_i\rho\right)\cos\theta \tag{1}$$

The different phases of the composite are identified with the subscripts 1 to 4, 1 representing the effective medium, i.e. the composite material as a whole, 2 the matrix attributed to a fibre, 3 the PyC interphase and 4 a fibre itself. Several parameters A_i and B_i can be set to zero for reasons discussed in the aforementioned papers [1,2]. As a result, Equation 2 can be written to describe the temperature fields in the various phases.

$$T_i = \begin{cases} \nabla T r\cos\theta & i = 1 \\ \left(\frac{B_i}{r} + C_i r\right)\cos\theta & 1 < i < 4 \\ C_i r\cos\theta & i = 4 \end{cases} \tag{2}$$

Using Neumann and Dirichlet boundary conditions at the domain interfaces, one can solve the resulting overdetermined equation system shown below:

$$r = b : \begin{cases} \nabla T = \frac{B_2}{b^2} + C_2 \\ k_1\nabla T = k_2\left(C_2 - \frac{B_2}{b^2}\right) \end{cases}$$

$$r = a + w : \begin{cases} \frac{B_2}{(a+w)^2} + C_2 = \frac{B_3}{(a+w)^2} + C_3 \\ k_2\left(C_2 - \frac{B_2}{(a+w)^2}\right) = k_3\left(C_3 - \frac{B_3}{(a+w)^2}\right) \end{cases}$$

$$r = a : \begin{cases} \frac{B_3}{a^2} + C_3 = C_4 \\ k_3\left(C_3 - \frac{B_3}{a^2}\right) = k_4 C_4 \end{cases}$$

From these, two expressions are obtained for the constant C_4. Equating these to one another yields an expression for k_1, the thermal conductivity of the composite, noted k_{eff}.

$$k_{eff} = k_m \left\{ (1-R_f)\left[1 - \frac{1}{\mu V_f} + R_m\left(1+\frac{1}{\mu V_f}\right)\right] - (1+R_f)\left[\mu(1-R_m) - \frac{1+R_m}{V_f}\right]\right\} / \left\{(1+R_f)\left[\mu(1-R_m) + \frac{1+R_m}{V_f}\right] - (1-R_f)\left[1 + \frac{1}{\mu V_f} + R_m\left(1-\frac{1}{\mu V_f}\right)\right]\right\} \quad (3)$$

The following variable changes have been made to obtain Equation 3:

$$\mu = \left(\frac{a+w}{a}\right)^2 \qquad \lambda = \left(\frac{b}{a}\right)^2 \qquad R_m = \frac{k_3}{k_2} \qquad R_f = \frac{k_3}{k_4}$$

Additionally, one needs to account for porosity effects so that the model is accurate. Based on microstructural observations, all of the porosity is found in the SiC matrix. Indeed, the fibres are close to theoretical density and their thermal conductivities have been well documented[11]. Several models can be applied to porous ceramics, a good review on this topic has been published by Smith and al.[12], in which the Landauer model[13] is evidenced as being the most appropriate at describing 15 to 60% porous ceramics.

$$k = \frac{1}{4}\left\{k_p(3\nu_p - 1) + k_s(2-3\nu_p) + \left\{[k_p(3\nu_p-1) + k_s(2-3\nu_p)]^2 + 8k_s k_p\right\}^{\frac{1}{2}}\right\} \quad (4)$$

Here, k_p is the pore thermal conductivity, a term that is usually non-zero. This part of heat transport has two components, a radiant and a gaseous fraction. The thermal radiation component depends on the optical properties of the material and arises from the emission of infrared radiation within the cavity, which contributes to the overall conductivity. Similarly, if the pore is filled with a conductive gas, it will also contribute to the overall heat transfer.

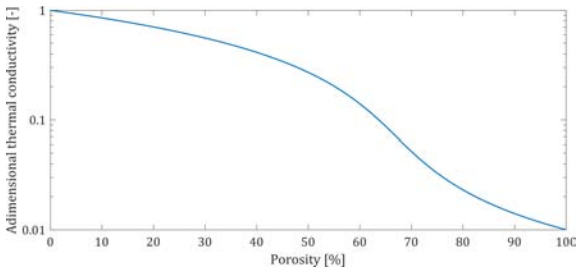

Figure 3: Relative reduction of the thermal conductivity due to porosity according to the Laundauer model. Calculation for a negligible k_p of one hundredth of k_m.

2.2. Thermal resistance series

The second *scale* at which the material has to be modelled is that of the cladding tube itself. This is rather straightforward since the multiple layers of the tube act as thermal barrier put in a series.

The thermal resistance of a single cylindrical shell of material is given by Equation 5:

$$R = \frac{ln\left(\frac{r_{\text{out}}}{r_{\text{in}}}\right)}{2\pi k L} \quad (5)$$

The total resistance arising from the stacking of N layers is obtained from Kirchoff's laws. Since the heat flux is perpendicular, the system is equivalent to a series circuit, i.e. the total resistance is the sum of all the layers resistances. Figure 4 shows a drawing of this situation and the thermal resistance of the whole tube is given by Equation 6.

$$R_{tot} = \sum_{i=1}^{N} \frac{\ln\left(\frac{r_{i+1}}{r_i}\right)}{2\pi k l} \quad (6)$$

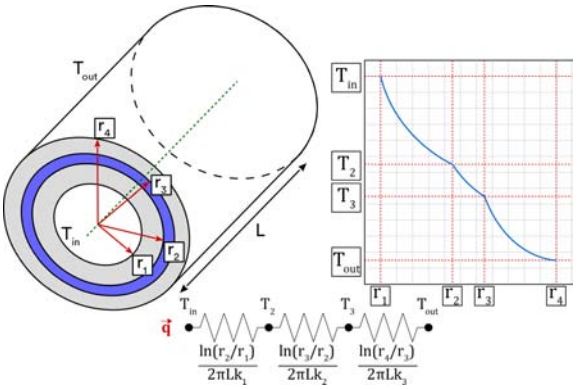

Figure 4: Sketch of a multilayered composite tube with the resulting network of thermal resistances as well as the general shape of the temperature profile if it were to be heated from the inside.

Using Equation 6, one can the extract an *equivalent* thermal conductivity for a composite cylinder made of N layers, given by Equation 7.

$$k_{eq} = \frac{\prod_{i=1}^{N} k_i \ln\left(\frac{r_N}{r_1}\right)}{\sum_{i=1}^{N}\left[\prod_{j\neq i}^{N} k_j \ln\left(\frac{r_{i+1}}{r_i}\right)\right]} \quad (7)$$

3. Results

Combining both the Landauer porosity model and the Markworth continuous medium approach, one can calculate the loss of thermal conductivity caused by amorphisation of the PyC interphase. Figure 5 shows the data resulting from such calculations for different porosity levels.

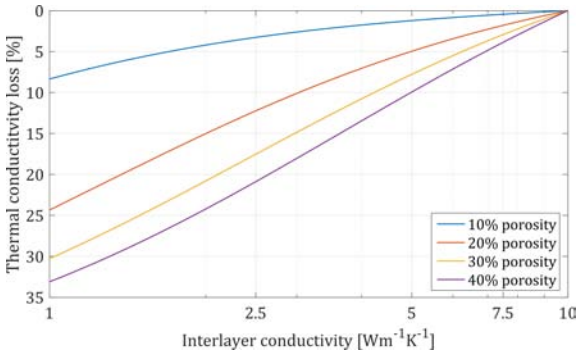

Figure 5: Effective thermal conductivity of a SiC/SiC composite with varying matrix porosity and interlayer thermal conductivity.

As one can see, a full amorphisation of the PyC interphase could lead to a decrease of 10 to 35%, depending on the amount of pores. The typical range of porosities in CVI SiC matrices is between 10 and 25% in average, with locally much higher porosities reaching 40 to 50%. Note that these results hold for a material in which the pores are insulators compared to the matrix.

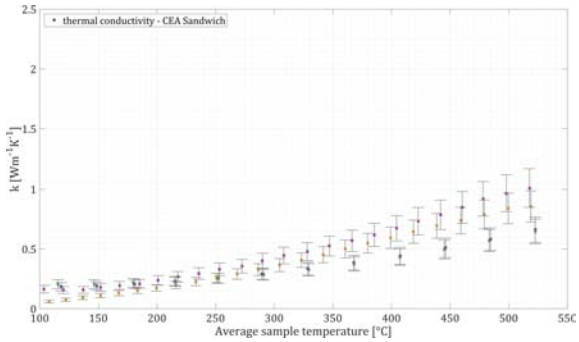

Figure 6: Radial heat flow thermal conductivity measurements carried out on CEA sandwich cladding tubes.

Figure 6 shows a thermal conductivity measurements carried out on SiC/SiC cladding tubes designed by the french CEAEA (Comissariat à l'Énergie Atomique et aux Énergies Alternatives). These samples feature a *sandwich* architecture, whereby a metallic liner made of tantalum is pressed between an inner and an outer layer or ceramic matrix composite.

The results featured in Figure 6 can appear surprisingly low compared to the data most are used to seeing as far as the thermal conductivity of SiC/SiC is concerned. The reason for the significant difference with usual literature results is explained by the following points.

- Firstly, these measurements have been carried out on 20 cm long sections of actual prototypes, i.e. non-ideal systems made of pure SiC/SiC layers. Figure 7 shows the cross-section of one of these samples, on the basis of which one can conclude that the end product is very inhomogeneous.

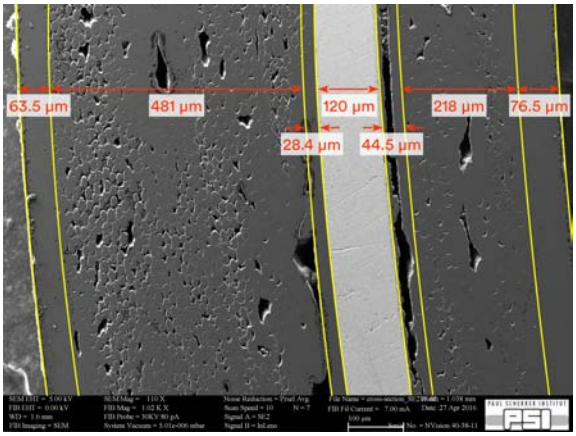

Figure 7: SEM image showing the microstructure of the cross-section of a CEA cladding tube section.

- Second, a large number of layers are involved, each acting as barriers of varying strengths against the radial heat flow. As one can see in Figure 7, these layers are far from being ideal, especially at the inner metal/ceramic interface. Indeed, this particular interface shows almost no contact between these two materials, meaning that very little heat transfer will occur there.

Another seemingly surprising result is the trend of increasing thermal conductivity as the measurement temperature elevates. This is due to the aforementioned thermal transport due to the forward scattering of infrared photons. Indeed, the fibres and pores have sizes close to the wavelength of IR radiation, meaning that significant scattering occurs in the Mie regime. Additionally, SiC is partially transparent to IR, meaning that though it will be limited since the material is finely grained, phonon diffusion within the material can occur as well. The increase featured on Figure 6 could not be explained by an early onset of electronic conduction. The width of the gap between the valence and conduction bands in cubic SiC is 2.36 eV at 300 K[14], which corresponds to a photon temperature of more than 10'000 K. However, the actual onset of electronic heat transport would occur at lower temperatures thanks to Boltzmann statistics.

Using Equation 7 and combining it with the aforementioned Landauer/Markworth approach to tackle the question of the thermal conductivity of the SiC/SiC layers allows one to determine the actual conductivity of the multilayer system. Figure 8 shows the temperature profile across the sample wall, considering the seven layers identified in the SEM image shown in Figure 7.

The profile displayed above shows that poorly adhered layers such as the ceramic/tantalum interface result in a quasi total insulation. Looking at the cross-section, we see that this layer shows only 10 to 20% of contact area with

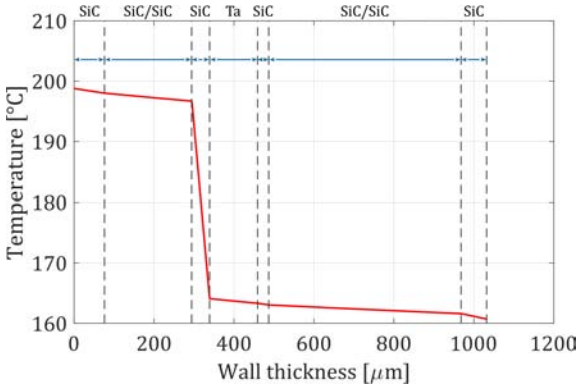

Figure 8: Temperature profile across the wall of a multilayered sandwich cladding with a structure such as the one feature in Figure 7.

the tantalum. Hence, the tube equivalent thermal conductivity is about 0.33 $W \cdot m^{-1} \cdot K^{-1}$. Though the overall porosity of the cladding tube is about 20%, the innermost and outermost layers are made of monolithic SiC, whose density can be considered practically equal to the theoretical 3.125 $g \cdot cm^{-3}$. Considering this as well as the fact that the metal liner is a purely dense component whose density is about 16.5 $g \cdot cm^{-3}$, the actual porosity of the SiC/SiC layers is closer to 25%.

4. Conclusions

In this paper, an effective theoretical modelling method based on a Markworth [1] continuous medium approach has been used as a basis in which the effects porosity, as well as those of microstructural features observed by SEM on cross-sections of prototype cladding tubes can be included. This modelling procedure makes it possible to understand the reasons why measurements carried out using a radial heat flow apparatus presented at the ANS 2016 annual meeting [4] show thermal conductivities much lower than what is common place from laser-flash data obtained from SiC/SiC discs.

The model also has the capability to include the effect of amorphisation of the PyC interphases, a radiation damage effect which has been observed by using EFTEM and STEM-EELS[1]. As shown in Figure 5, a fully amorphised PyC interlayer would induce a thermal conductivity loss of 10 to 35%, depending on the total composite porosity. However, this effect could not be evidenced from thermal conductivity measurements since samples made of a single layer of SiC/SiC would be required in both pristine and irradiated sates.

To conclude, we have shown that designs featuring many layers will have a low overall thermal conductivity due to interfacial thermal resistance. This is exacerbated by having poor adhesion between some of the layers, with significant issues in the case where metallic liners are being used for tightness purposes.

[1] This data has not been published yet.

5. Acknowledgements

The authors would like to acknowledge the GIF VHTR, CARAT (DE-NE0000566), EU Fp7 MaTISSE project (EU grant n°604862) and MeAWaT (ccem.ch/meawat) projects for funding this works as well as CEA and General Atomics for supplying samples.

References

[1] A. J. Markworth, The transverse thermal conductivity of a unidirectional fibre composite with fibre-matrix debonding: a calculation based on effective-medium theory, Journal of Materials Science Letters 12 (19) (1993) 1487–1489. doi:10.1007/BF00277073.

[2] G. E. Youngblood, D. J. Senor, R. H. Jones, Optimizing the transverse thermal conductivity of 2D-SiCf/SiC composites. I. Modeling, Journal of Nuclear Materials 307–311, Part 2 (2002) 1112–1119. doi:10.1016/S0022-3115(02)00951-0.

[3] D. Flynn, A radial-flow apparatus for determining the thermal conductivity of loose-fill insulations to high temperatures, Journal of Research of the National Bureau of Standards-C. Engineering and Instrumentation 67C (2) (1963) 129–137.

[4] L. Fave, M. Pouchon, A Radial Heat Flow Apparatus For Thermal Conductivity Characterisation of Cylindrical Samples, Vol. ANS Transactions - volume 14, American Nuclear Society, 555 North Kensington Avenue, La Grange Park, IL 60526 (United States), New Orleans, Louisiana, USA, 2016.

[5] K. Wen, J. Marrow, B. Marsden, Microcracks in nuclear graphite and highly oriented pyrolytic graphite (HOPG), Journal of Nuclear Materials 381 (1–2) (2008) 199–203. doi:10.1016/j.jnucmat.2008.07.012.

[6] W. Bollmann, G. R. Hennig, Electron microscope observations of irradiated graphite single crystals, Carbon 1 (4) (1964) 525–533. doi:10.1016/0008-6223(64)90015-6.

[7] R. H. Telling, C. P. Ewels, A. A. El-Barbary, M. I. Heggie, Wigner defects bridge the graphite gap, Nature Materials 2 (5) (2003) 333–337. doi:10.1038/nmat876.

[8] R. H. Telling, M. I. Heggie, Radiation defects in graphite, Philosophical Magazine 87 (31) (2007) 4797–4846. doi:10.1080/14786430701210023.

[9] A. A. Balandin, Thermal properties of graphene and nanostructured carbon materials, Nature Materials 10 (8) (2011) 569–581. doi:10.1038/nmat3064.

[10] L. R. F.R.S, XXXI. Investigations in optics, with special reference to the spectroscope, The London, Edinburgh, and Dublin Philosophical Magazine and Journal of Sciencedoi:10.1080/14786447908639684.

[11] J. A. DiCarlo, H.-M. Yun, Non-oxide (Silicon Carbide) Fibers, in: N. P. Bansal (Ed.), Handbook of Ceramic Composites, Springer US, 2005, pp. 33–52. doi:10.1007/0-387-23986-3_2.

[12] D. S. Smith, A. Alzina, J. Bourret, B. Nait-Ali, F. Pennec, N. Tessier-Doyen, K. Otsu, H. Matsubara, P. Elser, U. T. Gonzenbach, Thermal conductivity of porous materials, Journal of Materials Research 28 (17) (2013) 2260–2272. doi:10.1557/jmr.2013.179.

[13] R. Landauer, The Electrical Resistance of Binary Metallic Mixtures, Journal of Applied Physics 23 (7) (1952) 779. doi:10.1063/1.1702301.

[14] Y. Goldberg, M. Levinshtein, S. Rumyantsev, Silicon Carbide (SiC), in: M. Levinshtein, S. Rumyantsev, M. Shur (Eds.), Properties of Advanced Semiconductor Materials: GaN, AIN, InN, BN, SiC, SiGe, john wiley & sons, inc. Edition, Wiley, New York, 2001, pp. 93–148.